

Aya M.E. AHMED<sup>1</sup>  <https://orcid.org/0000-0002-8636-4598>

Osman HAMDY<sup>2</sup>  <https://orcid.org/0000-0002-4397-9015>

Youssef L.Z. SAAD<sup>3</sup>  <https://orcid.org/0000-0003-0182-0329>

Seleem S.E. AHMAD<sup>4</sup>  <https://orcid.org/0000-0001-9894-0209>

<sup>1,2</sup>Zagazig Higher Institute of Engineering & Technology, Department of Civil Engineering,  
Zagazig, Egypt

<sup>3,4</sup>Zagazig University, Faculty of Engineering, Zagazig, Egypt

# Residual strength and toughness after impact loading for RC slabs strengthened with different layers of geogrid

**Keywords:** impact load, geogrid, RC slab, residual strength, static flexural load, toughness, toughness index

## Introduction

Concrete is very brittle under tensile stresses and impact loads, so reinforcing bars or pre-stressing steel are added. Augmented concrete slabs are the structural elements extensively used in building structures. Basic concrete components require materials such as glass, carbon, steel fibers and Geosynthetic composites, including geogrid and geocells, to improve their strength, stiffness, flexural resistance, as well as impact and abrasion resistance (Vijay, Raj & Babu, 2021). Geogrids are polymers, such as polyester, polypropylene, and polyethylene, and consist of regular rectangular, square or triangular apertures (Dong, Han & Bai, 2011). Three main types of geogrids are

used for reinforcement: uniaxial, biaxial, and triaxial (El Meski & Chehab, 2014). Many advantages lead to the use of geogrid, such as high resistance to attack by chlorides and sulfates, corrosion, being very light in terms of weight, relatively cheap, easy to transport, cut and use, and providing shear strength and high tensile resistance (Chidambaram & Agarwal, 2015; Yousif, Mahmoud, Abd Hacheem & Rasheed, 2021). Therefore, geogrid can replace tension steel in reinforced concrete elements (Nishanthi et al., 2021). Ibrahim, Turk and Fares (2020) scrutinize the effect of slab thickness on the mechanical behavior of high-strength concrete slabs containing geogrid as reinforcement layers. It was observed that the increase in the slab thickness from 50 to 80 mm led to an increase in the ultimate loads and the absorbed energy for the plain concrete control slab. Increasing slab thickness increased the slabs' ultimate loads for specimens reinforced using uniaxial, biaxial, and triaxial geogrid by about 216.3%, 100%, and 167.3%, respectively. Still, it decreased the absorbed energy for specimens reinforced using the biaxial and triaxial geogrid by about 22.5% and 16.75%, respectively. The study by Fares, Hassan and Arab (2020) considered the flexural behavior of high-strength concrete slabs reinforced with the treated and untreated geogrid. They found that using two layers of uniaxial and triaxial geogrid as reinforcement for ordinary concrete slabs gives lower results than biaxial geogrid. The maximum loading capacity of flexural behavior for the tested slab treated chemically increased by about 8.5% for one geogrid and 13% for two geogrids compared to the untreated samples. Moreover, the addition of the geogrid reduced the maximum flexural loading capacity, but substantially increased the flexibility of the slab. Geogrid may be an effective alternative material for concrete confining. Chidambaram and Agarwal (2014) studied the effect of geogrid confining on the mechanical properties of concrete samples reinforced with steel fiber under flexural and compression. They found that the geo-network power and number of layers played an essential role in enhancing deformation and crack propagation. Meng, Jiang and Liu (2021) studied previous concrete strength, permeability, and flexural behavior with various coarse aggregate sizes, geogrid positions and layers by experimentation. They found that geogrids improved the concrete beam's flexural strength, deformability and energy absorption capability. The optimum flexural behavior of the concrete beam was obtained by putting the geogrid at both one-third and two-thirds of the concrete heights. The geogrid was put in a suitable position in the previous concrete. Besides, the large size (10–15 mm) aggregates resulted in remarkable post-cracking performance, while the small size (5–10 mm) aggregates provided high flexural strength for the concrete beam. The study performed by Mohammed and Najim (2020) investigated the mechanical strength, flexural behavior and fracture energy by using aggregates of a recycled concrete (RCA) to make self-compacting concrete (RASCC).

It was concluded that the mechanical strength, including flexural, splitting, and compressive strengths was decreased by adding RCA with slight decline in the modulus of elasticity. However, this reduction of the required mechanical strength did not affect its use as structural concrete. Vijay, Kumar, Vandhiyan, Mahender and Tharani (2020) experimented with the impact behavior of the geogrid-reinforced concrete slabs. The experimental results showed that the RC slab samples reinforced with geogrid and steel had a superior performance by refining the resistance to the impacted shear stress, and this helped spread the tensile stress from the impact loading to a large area, thus evading the accumulation stress at a specific loading point. These specimens can withstand a higher number of impact loading blows, which affects the performance of impact energy absorption and impact ductility index. Muda et al. (2013) experimentally studied the behavior of the lightweight oil palm shells (OPS) concrete slab reinforced with geogrid of  $30 \times 30$  cm size with 2 cm, 3 cm, and 4 cm thick cast with various geogrid orientations and boundary conditions exposed to low impact projectile test. The results showed that using geogrid amplified the impact resistance and had good cracking resistance compared to the samples without geogrid. The orientation of the geogrid in the OPS concrete slab has little significance in the crack resistance. A worthy linear relationship exists between the ultimate and the first crack resistance against the thickness of the slab. Al Qadi, Al-Kadi, and Al-Zaidyeen (2015) studied the impact resistance of oil-palm shells (OPS) experimentally on lightweight concrete slabs reinforced with a geogrid. Adding a geogrid layer in the sample raised the cracking resistance, both for the first crack and the ultimate failure. Geogrid 80/80, with a characteristic short-term tensile strength of  $80 \text{ kN}\cdot\text{m}^{-1}$  in both directions, had a better impact on cracking resistance. Yahaghi, Muda and Beddu (2016) studied the impact resistance of the oil palm shells (OPS) concrete reinforced with the polypropylene (PP) fiber. There was a strong linear relationship between the volume fraction of the PP fiber, impact resistance and cracking resistance ratio. This relation was unbeatable by any change in the thickness from 20 to 40 mm. Although the thickness increment enhanced the impact resistance meaningfully, the effect was more obvious for ultimate failure crack resistance than for first crack resistance. Ahmad, Seleem, Badaway and El Safoury (2016) studied the behavior of high-performance concrete slabs supported by steel and polypropylene fiber under flexural impact loading. The used specimen was slab of dimensions  $500 \times 500 \times 60$  mm reinforced with 10 mm diameter steel bars in two directions. They found that there were fully damaged ones that took place among the specimens under impact from height of 270 cm. While partial damage had happened for impacted specimens from height 80 cm and can be tested under central flexural test the residual strength was different according to fiber type and content. Ganesh, Muthukannan, Dhivya, Sangeetha and Daffodile (2020)

studied the mechanical properties of hybrid fiber-reinforced geopolymer concrete specimens. The polypropylene fibers and the glass were added in several quantities. They found that using 1% polypropylene fiber produced maximum toughness index values. They used 1% glass fiber to produce maximum stiffness under yield and ultimate strain conditions. Ye, Liu, Zhang, Wang and Peng (2020) carried out an experiment to study the effect of high-strength steel fiber lightweight aggregate concrete (HSLAC) on the mechanical properties together with the toughness index. Three types of steel fibers were studied, and these were: being micro (M), end-hooked (H), and corrugated (C), and they were the proportions of the studied fiber content 0.5–2.0%. The M steel fibers reinforcement had the best results on the mechanical properties. It had the best toughness value with the same fiber content. Furthermore, the toughening effect of H and C steel fibers could only reach 66% and 50% of M steel fibers, respectively. Su and Fan (2021) studied the flexural toughness of steel–polyvinyl alcohol hybrid fiber reinforced. The results proved that the concurrent integration of the steel fiber and polyvinyl alcohol fiber critically improved the concrete's maximum load and the toughness index throughout bending failure, while fiber concrete had a noticeable strain-hardening phenomenon. When polyvinyl alcohol fiber volume content is 0.75% and steel fiber volume content is 1.25%, hybrid fiber concrete shows a good positive hybrid effect, which is perfect for advancing the bending performance. Ou, Tsai, Liu and Chang (2012) studied the properties of the compressive stress–strain behavior of steel fiber-reinforced concrete (SFRC) with a high reinforcing index. They found that the toughness of concrete increased with a fiber volume fraction equal to 2% when using steel fibers. Also, longer fibers increased the toughness of concrete more than the short ones. In this work, an experimental study carried out for three groups of reinforced concrete slabs of different thicknesses supported by biaxial geogrid layers at different distances, and each group contained six slabs. In each group, ultimate load, deflections, toughness, and toughness index were measured while testing specimens.

## Experimental program

Table 1 shows the different configurations of the geogrid reinforcement used of the RC slabs studied in the current work. Each RC slab was reinforced by 5Ø10/m as lower steel reinforcement in both directions. The dimensions of the slabs were 50 × 50 cm, where three different thicknesses considered 12 cm, 15 cm and 18 cm. Moreover, different locations from the upper face of concrete were considered in the current study.

TABLE 1. Configurations of tested RC slabs

Slab thickness ( <i>t<sub>s</sub></i> ) [cm]	Geogrid configuration	Test condition	Location from upper face ( <i>CC</i> ) [cm]
12	without	static, control	–
	one layer	static, control	3
	one layer	impact	3
	two layers	impact	3
	one layer	impact	5
	two layers two layers	impact impact	5 3 and 6
15	without	static, control	–
	one layer	static, control	3
	one layer	impact, static	3
	two layers	impact, static	3
	one layer	impact, static	5
	two layers two layers	impact, static impact, static	5 3 and 7.5
18	without	static, control	–
	one layer	static, control	3
	one layer	impact, static	3
	two layers	impact, static	3
	one layer	impact, static	5
	two layers two layers	impact, static impact, static	5 3 and 9

Source: own work.

Each slab sample was casted in timber mold painted with oil with inner dimensions of 50 × 50 cm with 5Ø10/m as lower steel reinforcement in both directions. The mold sides were in timber with a thickness of 2.5 cm, whereas the bottom timber side was 0.5 cm, the geogrid reinforcement layers added at their position in accordance with each case individually throughout the casting process.

## Tests preparation

### Material

Material properties of the concrete used, steel reinforcement, and geogrid reinforcement were precisely measured before the experiment. The mix design of the used concrete is shown in Table 2, together with the average compressive strength of tested three standard cubes with dimensions of 15 × 15 × 15 cm.

TABLE 2. Concrete trail mix proportions of concrete mixes

Concrete ingredient	Unit	Dosage value
Cement	$\text{kg}\cdot\text{m}^{-3}$	300
Water	$\text{l}\cdot\text{m}^{-3}$	160
Gravel	$\text{kg}\cdot\text{m}^{-3}$	1 120
Sand	$\text{kg}\cdot\text{m}^{-3}$	720
The average result of three cubes of compressive strength	$\text{kg}\cdot\text{cm}^{-2}$	252

Source: own work.

TABLE 3. Properties of biaxial geogrid

Index properties	Unit	Value
Aperture dimensions from center to center	cm	3.7
Rib thickness	cm	0.2
Tensile strength	$\text{kN}\cdot\text{m}^{-2}$	30
Elongation	%	11
Weight	$\text{g}\cdot\text{m}^{-2}$	320
Roll width	cm	50
Roll length	cm	400

Source: own work.

A tension test, according to the Egyptian ES 262-2/2015 standard (Egyptian Organization for Standardization & Quality [EOS], 2015), and ISO 6935-2/2007 standard (International Organization for Standardization [ISO], 2007), were done for the reinforcement steel bars. Three samples were tested. The average results for reinforcement were 411 MPa as yield strength, 633 MPa as tensile strength and 15% as maximum elongation. Moreover, the geometric and strength properties of the geogrid reinforcement used, as recommended by the manufacturer, are given in Table 3.

## Casting and curing

Mixing the concrete components was done by a mechanical mixer, then casted and placed in layers inside the mold. The compaction for the unreinforced slab by geogrid, control specimen, was done completely by using a mechanical vibrating table. On the other hand, for slabs reinforced by geogrid layers, we used a combination of a vibrating table and manual compaction so that we kept the geogrid layer at a distance during fixing, as shown in Figure 1. After that, the surface was finished and flattened.

Plastic sheets were used to cover the slab samples and cubes for 24 h, as shown in Figure 2, and all samples were unmolded and labeled. The cubes were submerged in clean water for 28 days as a curing process before performing the compression test as shown in Figure 3. The average result of the three cubes of compressive strength is 25.2 MPa.

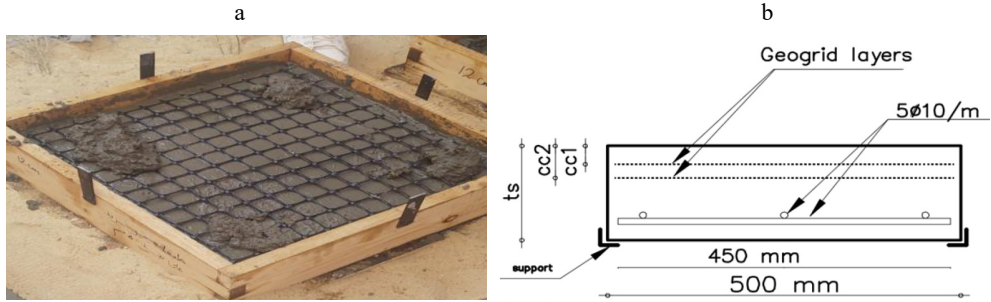


FIGURE 1. Placing a geogrid layer through the casting process (a) and schematic figure for tested specimens (b)

Source: own work.



FIGURE 2. Labeled RC samples after unmolding

Source: own work.



FIGURE 3. Compression test

Source: own work.

## Tests

### Impact test

A special impact testing machine was designed and fabricated at the laboratories in the Faculty of Engineering, Zagazig University by Seleem, Mohamed, Aml and Ashraf and Safoury in 2016, considering the drop weight impact test mechanism. The impact-testing machine can perform flexural impact tests for  $50 \times 50$  cm slabs with different thicknesses. The components of the impact-testing machine are detailed in Figure 4b.

The machine steel frame was fabricated from steel sections considering the mechanism of dropping weight to act as rails to ensure the direction of the drop is in the specimen's center. The drop weight weighs 70 kg. The dropping weight is elevated

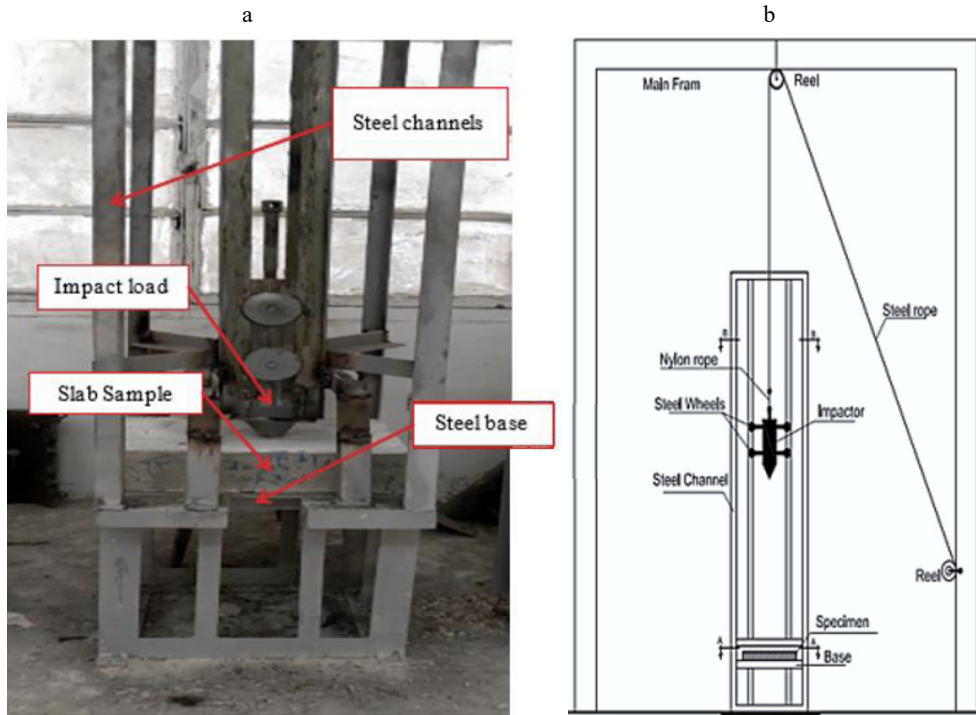


FIGURE 4. Set up of the impact test (a); impact testing machine components (b)

Source: own work.

up to the specified height (150 cm), using a steel cable hung on a steel wheel at the top of the frame, as shown in Figure 4b. The drop weight is changed by moving the wheel arm to pull the steel cable to the specified height. After dropping the impactor, it released from the specimen and was fixed for the next drop; the number of drops for each specimen is five.

### Static and residual load test

After subjecting the slabs to the impact load (Fig. 4), the residual strength is determined by loading the slabs with the static load (Fig. 5). As residual strength refers to the ability of a material or structure to resist further damage and maintain its load-carrying capacity even after experiencing some level of damage due to pre-loading. The residual load is here determined by exposing the samples to an impact test under a load of 70 kg, dropped from a height of 150 cm, and subjected to five blows, then exposing the samples again to the flexural test, and then the load is recorded (residual load).

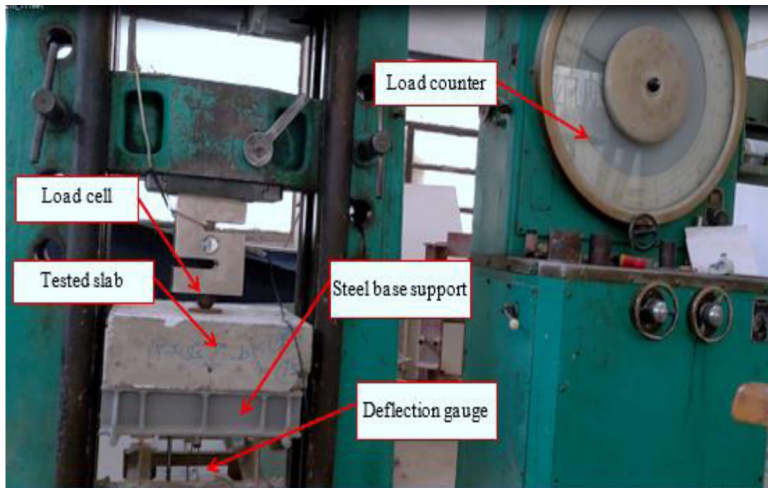


FIGURE 5. Set up of the static test

Source: own work.

The load and deflection are recorded through different stages of the loading process during the slab loading centrally. The static applied load of the test machine was concentrated on the center point using a hard steel ball with a 30 mm diameter on the top face of the specimen, as shown in Figure 4a. White water paint was used to paint the bottom face of the slab; this face was divided into squares  $100 \times 100$  mm to notice the crack pattern during and after the static loading test.

## Results and discussion

### Control specimens

Six control samples with/without geogrids are subjected directly to a static load test without any impact for comparison. The load and deflection relation are recorded through a static loading process for all specimens. Figures 6–8 show the load–deflection curves for control 12 cm, 15 cm, and 18 cm control specimens with/without geogrid.

As shown in Figures 6–8, the specimens with a geogrid showed more loading capacity and maximum deflection than slabs without geogrids. Where for 12 cm thick slabs, the maximum load was enhanced from 95 kN to reach 103 kN and the maximum deflection increased from 2.714 mm to 5.486 mm. For 15 cm thick slabs, the maximum load was enhanced from 122 kN to reach 150.12 kN, and the maximum

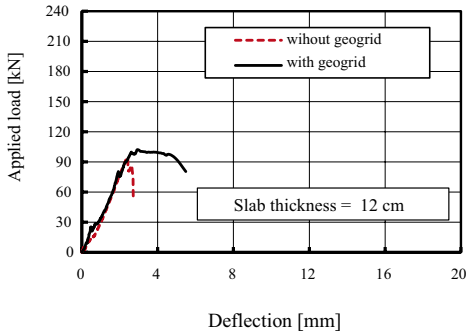


FIGURE 6. Load against deflection for control slab with thickness of 12 cm

Source: own work.

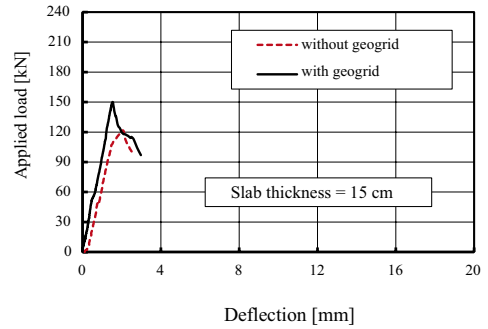


FIGURE 7. Load against deflection for control slab with thickness of 15 cm

Source: own work.

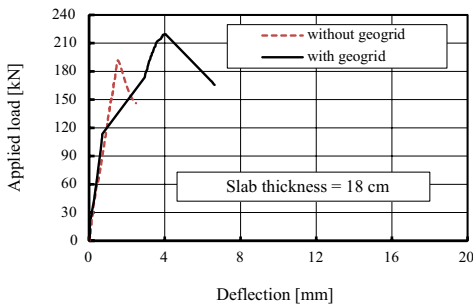


FIGURE 8. Load against deflection for control slab with thickness of 18 cm

Source: own work.

deflection was increased from 2.53 mm to reach 2.983 mm. Also, for 18 cm thick slabs, the maximum load was enhanced from 192 kN to reach 220 kN, and the maximum deflection was increased from 2.478 mm to reach 6.633 mm. These results confirmed the positive effect of geogrid reinforcement on the slab strength and toughness. Moreover, the data indicated that the slab toughness enhancement was due to the existence of a geogrid with the increasing slab thickness.

## Failure mode of control specimens

Figures 9–12 illustrate a comparison of the failure modes and crack pattern for the tested control specimens with geogrid and without geogrid under static loads only. The Figures show that a geogrid effectively affects the crack pattern and distribution, especially for thickness of 12 cm and 18 cm.

By comparing the crack behavior for all specimens, it is clear that the geogrid affects the number of cracks, as samples containing the geogrid reduce the number and distribution of cracks and mitigate their severity. It is clear that the geogrid samples have an optimal fracture pattern and distribution due to good resistance to flexural load and high values of ultimate loads than samples without geogrid, which comply with the previous load deflection figures.

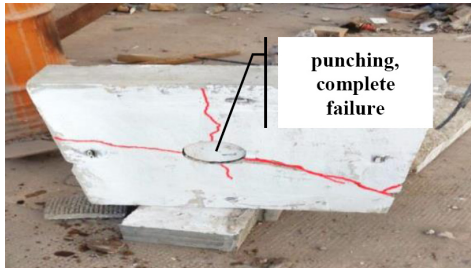


FIGURE 9. Failure mode of control specimen t12 without geogrid under static loads only  
Source: own work.

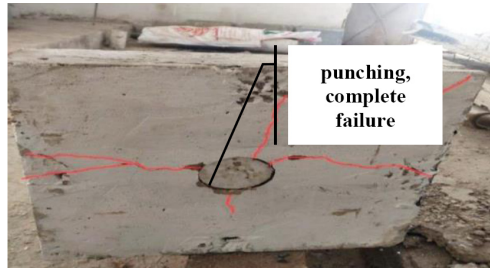


FIGURE 10. Failure mode of control specimen t12 with one-layer geogrid under static loads only  
Source: own work.

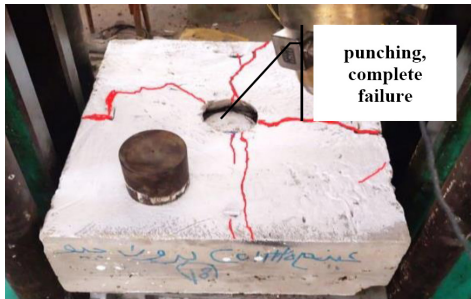


FIGURE 11. Failure mode of control specimen t18 without geogrid under static loads only  
Source: own work.



FIGURE 12. Failure mode of control specimen t18 with one-layer geogrid under static loads only  
Source: own work.

## Impact test results

The test was conducted on 15 slabs ( $50 \times 50$  cm) of different thicknesses (12 cm, 15 cm and 18 cm). All samples were tested under a load of 70 kg, dropped from a height of 150 cm, and subjected to five blows. The slab samples with a thickness of 12 cm got completely damaged, as shown in Figures 13 and 14, so they were not tested by the static load test, i.e., their residual strength equals.

Table 4 shows the number of drops required for full damage for 12 cm slabs. The results showed that slabs reinforced with one layer of geogrid are stronger than slabs reinforced with two layers for 12 cm.

The slabs with a thickness of 15 and 18 cm did not have complete damage, so a static flexural test was performed for them. Figures 13–16 show some details of failure for slabs after being subjected to impact load with thicknesses of 12 cm, 15 cm and 18 cm, respectively.



FIGURE 13. Failure pattern of 12 cm slabs with two layers of geogrid at 3 cm after impact loading  
Source: own work.

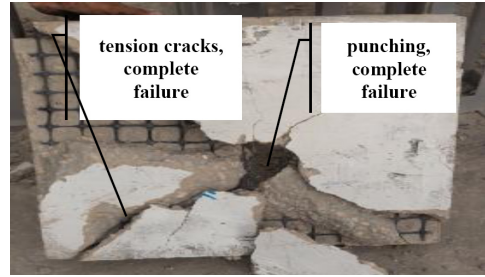


FIGURE 14. Failure pattern of 12 cm slabs with one layer of geogrid at 5 cm after impact loading  
Source: own work.



FIGURE 15. Failure pattern of 18 cm slabs with two layers of geogrid at 3 cm after impact loading  
Source: own work.



FIGURE 16. Failure pattern of 15 cm slabs with two layers of geogrid at 5 cm after impact loading  
Source: own work.

TABLE 4. Number of drops for full damage for 12 cm slabs

Sample case	Drops for full damage
t12 one layer of 3 cm	5
t12 one layer of 5 cm	5
t12 two layers of 3 cm	4
t12 two layers of 5 cm	4
t12 two layers of 3 and 6 cm	4

Source: own work.

### Residual static test results

The results of the residual static tests are recorded for each slab in the form of a relation between static loads with its corresponding deflection. As mentioned before, the load is concentrated in each slab’s center, where the deflection is recorded for the same point of the slab center. Figures 17 and 18 show the residual load–deflection curves of each sample under static load, whereas, as shown from the graphs, the load–deflection relation proceeds a positive linear relation at the first stage until reaching the maximum load, followed by a nonlinear negative relation till complete failure.

The results of the residual static tests are recorded for each slab in the form of a relation between static loads with its corresponding deflection. As mentioned before, the load is concentrated in each slab’s center, where the deflection is recorded for the same point of the slab center. Figures 17 and 18 show the residual load–deflection curves of each sample under static load, whereas, as shown from the graphs, the load–deflection relation proceeds a positive linear relation at the first stage until reaching the maximum load, followed by a nonlinear negative relation till complete failure.

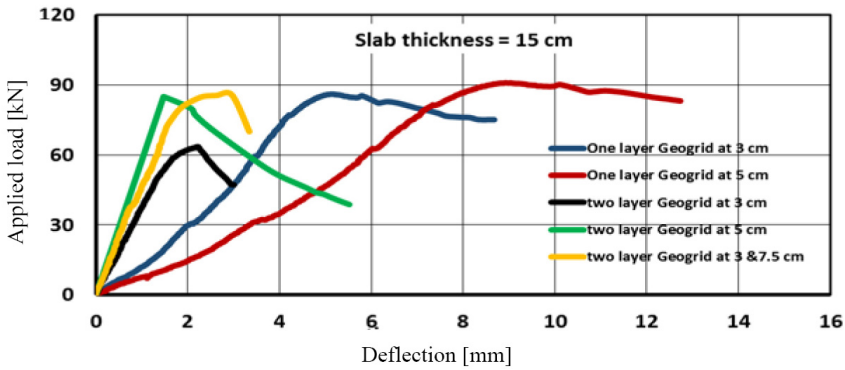


FIGURE 17. Residual load against deflection for slab with thickness of 15 cm with geogrid  
Source: own work.

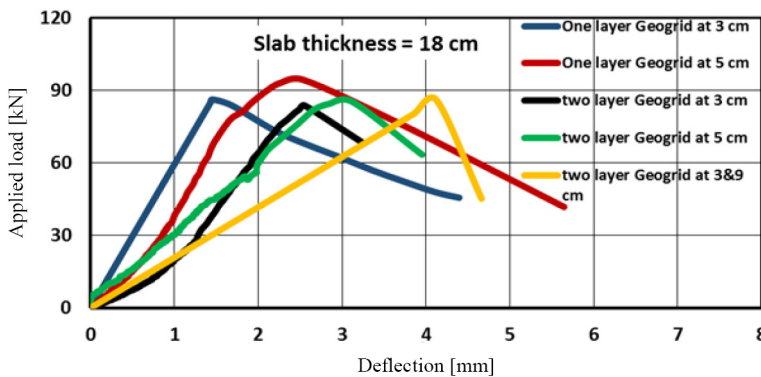


FIGURE 18. Residual load against deflection for slab with thickness of 18 cm with geogrid  
Source: own work.

The maximum load, maximum deflection, deflection at maximum load, toughness, and toughness index for each specimen are shown in Table 5 for comparison. Also, Table 5 shows the deflection at maximum load, maximum deflection, toughness index, and toughness for each sample separately.

As shown in Table 5, the residual strength value increased by increasing the slab thickness value or location of geogrid from the upper face of the slab. On the other hand, the higher number of geogrid layers, the lower the residual strength value. Moreover, the results in Table 5 also show that the higher the slab thickness or the number of geogrid layers, the lower the toughness value. Three control samples were considered in this study; the control slabs contain one layer of geogrid

TABLE 5. Results of residual test

Sample case	Maximum load ( $P_{max}$ ) [kN]	Deflection at maximum or cracked load [mm]	Maximum deflection ( $\Delta_{max}$ )	Toughness index at maximum load ( $\Delta_{max}/\Delta$ )	Toughness [kN·mm]
t15 one layer of 3 cm	86.07	5.18	8.676	1.674	502.673
t15 one layer of 5 cm	90.90	9.04	12.730	1.408	732.607
t15 two layers of 3 cm	63.50	2.21	3.006	1.358	130.980
t15 two layers of 5 cm	85.00	1.48	5.521	3.742	303.580
t15 two layers of 3 and 7.5 cm	85.77	2.96	3.342	1.128	288.908
t18 one layer of 3 cm	86.28	1.45	4.394	3.030	250.940
t18 one layer of 5 cm	94.50	2.53	5.645	2.232	349.328
t18 two layers of 3 cm	83.79	2.55	3.236	1.269	145.824
t18 two layers of 5 cm	85.50	3.11	3.951	1.270	244.914
t18 two layers of 3 and 9 cm	86.00	4.13	4.661	1.130	212.616

Source: own work.

with a 3 cm upper concrete cover for slabs with thicknesses of 12 cm, 15 cm, and 18 cm. Since the 12 cm slab already damaged in the impact process so the 12 cm, control slab ignored.

The control samples were subjected to the static load test without the impact test. Its results were compared with the same corresponding impact samples, i.e., samples subjected to impact loading before the static test. Figures 19 and 20 show the static load–deflection curves for control and corresponding samples exposed to impact for both 15 and 18 slabs containing one geogrid layer with a 3 cm upper concrete cover.

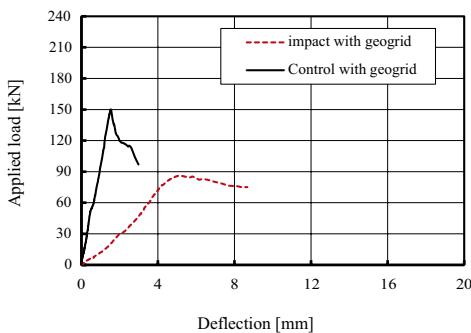


FIGURE 19. load against deflection for slab with thickness of 15 cm with one layer of 3 cm and control case

Source: own work.

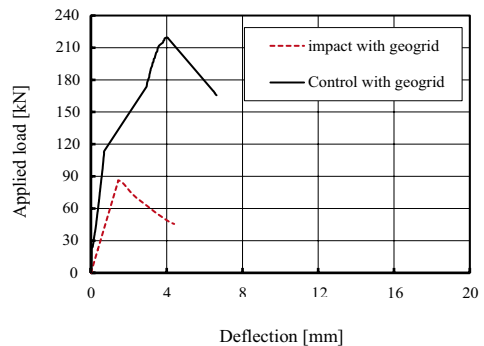


FIGURE 20. load against deflection for slab with thickness of 18 cm with one layer of 3 cm and control case

Source: own work.

Figures 19 and 20 clearly show the effect of exposing the slabs to five times the impact load on the residual load test. The residual strength ratio is calculated as a percentage value of the maximum load capacity of the samples exposed to impact loads compared to the maximum load capacity of the control samples that were exposed to static load tests only. The  $50 \times 50$  cm slabs exposed to a five-time drop 70 kg load from 150 cm have residual forces equal to 48.6% and 48.0% for 15 cm and 18 cm slabs, respectively, of the maximum failure load capacity.

### Failure modes for residual load test

This test was performed for samples that were not completely damaged after the impact test from a height of 150 cm. Figures 21–24 illustrate the mode of fracture for tested specimens under a central flexural load after the impact test. The cracks during residual test are continuing from cracks generated during the impact test or newly generated cracks during the residual test. These figures show that the number and distribution of these cracks are clearly different according to the number and location of the geogrid layers and thicknesses of the slabs.

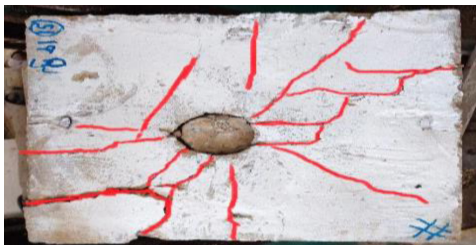


FIGURE 21. Failure mode of specimen with t15 and one layer of geogrid at 5 cm  
Source: own work.

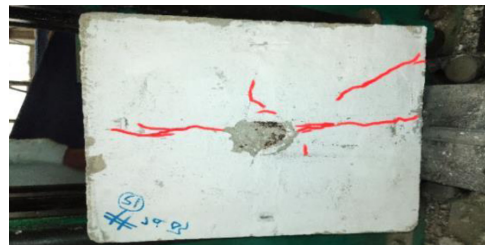


FIGURE 22. Failure mode of specimen with t15 and two layers of geogrid at 5 cm  
Source: own work.



FIGURE 23. Failure mode of specimen with t18 and one layer of geogrid at 5 cm  
Source: own work.



FIGURE 24. Failure mode of specimen with t18 and two layers of geogrid at 5 cm  
Source: own work.

As shown from previous Figures, more slab thickness, fewer cracks' numbers or length, more geogrid layers, fewer cracks' numbers or length occurred, especially for double layers with the same concrete cover.

## Conclusions

The subsequent conclusions from this experiment are:

1. The increase in the slab thickness gives an enhancement in the strength and residual strength.
2. Moreover, as the location of geogrid from the slab's upper surface increased, the strength, residual strength, and toughness improved.
3. The higher numbers of geogrid layers have a negative effect on the strength.
4. The higher the slab thickness or the number of geogrid layers, the lower the toughness value.
5. The residual strength of the slabs reinforced with upper geogrid after the impact test equals around 48% of the maximum failure load of the same slab.
6. A geogrid reduced the number and distribution of cracks and mitigated their severity more than that of specimens without a geogrid, especially for double layers with the same concrete cover.
7. Because of no rust in geogrids, that allows putting geogrid very near the surface, which leads to a greater capability of shrinkage resisting and preventing surface cracks.

## References

- Ahmad, S. S., Seleem, M. H., Badaway, A. A. & El Safoury, A. (2016). *Fracture and damage in high-performance concrete under impact loading*. Retrieved from: [https://www.researchgate.net/profile/SeleemAhmad/publication/279445985\\_Flexural\\_behavior\\_of\\_fiber\\_reinforced\\_concrete\\_slabs\\_under\\_central\\_impact\\_load/links/582abf3008aef19cb805fecd/Flexural-behavior-of-fiber-reinforced-concrete-slabs-under-central-impact-load.pdf](https://www.researchgate.net/profile/SeleemAhmad/publication/279445985_Flexural_behavior_of_fiber_reinforced_concrete_slabs_under_central_impact_load/links/582abf3008aef19cb805fecd/Flexural-behavior-of-fiber-reinforced-concrete-slabs-under-central-impact-load.pdf) [accessed: 30.01.2023].
- Al Qadi, A. N., Al-Kadi, Q. N. & Al-Zaidyeen, S. M. (2015). Impact strength of oil-palm shell on lightweight concrete slabs reinforced with a geo-grid. *Journal of Materials in Civil Engineering*, 27 (10), 04014264.
- Chidambaram, R. S. & Agarwal, P. (2014). The confining effect of geo-grid on the mechanical properties of concrete specimens with steel fiber under compression and flexure. *Construction and Building Materials*, 71, 628–637. <https://doi.org/10.1016/j.conbuildmat.2014.08.059>

- Chidambaram, R. S. & Agarwal, P. (2015). Flexural and shear behavior of geo-grid confined RC beams with steel fiber reinforced concrete. *Construction and Building Materials*, 78, 271–280. <https://doi.org/10.1016/j.conbuildmat.2015.01.021>
- Dong, Y. L., Han, J. & Bai, X. H. (2011). Numerical analysis of tensile behavior of geogrids with rectangular and triangular apertures. *Geotextiles and Geomembranes*, 29 (2), 83–91. <https://doi.org/10.1016/j.geotexmem.2010.10.007>
- Egyptian Organization for Standardization & Quality [EOS] (2015). *Steel for the reinforcement of concrete. Part 2: Ribbed bars* (ES 262-2/2015). Cairo: Egyptian Organization for Standardization & Quality [in Arabic].
- El Meski, F. & Chehab, G. R., (2014). Flexural behavior of concrete beams reinforced with different types of geogrids. *Journal of Materials in Civil Engineering*, 26 (8), 04014038. <https://ascelibrary.org/doi/10.1061/%28ASCE%29MT.1943-5533.0000920>
- Elsayed, A., Hamdy, O., Saad, Y. & Ahmad, S. (2023). Assessment of shrinkage strain reduction SSR for RC slabs with different thicknesses strengthen with different layers of geogrid. *The Egyptian International Journal of Engineering Sciences and Technology*, 41 (1), 48–55.
- Fares, A. E. R., Hassan, H. & Arab, M. (2020). Flexural behavior of high strength self-compacted concrete slabs containing treated and untreated geogrid reinforcement. *Fibers*, 8 (4), 23. <https://doi.org/10.3390/fib8040023>
- Ganesh, A. C., Muthukannan, M., Dhivya, M., Sangeetha, C. B. & Daffodile, S. P. (2020). Structural performance of hybrid fiber geopolymer concrete beams. *IOP Conference Series: Materials Science and Engineering*, 872 (1), 012155. <https://doi.org/10.1088/1757-899X/872/1/012155>
- Ibrahim, H. M., Turk, A. M. & Fares, A. M. (2020). Effect of slab thickness on the behavior of concrete slabs containing geogrid layers as reinforcement. *International Journal of Advanced Research in Science, Engineering and Technology*, 7 (7), 14999–14307.
- International Organization for Standardization [ISO] (2007). *Steel for the reinforcement of concrete. Part 2: Ribbed bars* (ISO 6935-2:2007). Geneva: International Organization for Standardization.
- Meng, X., Jiang, Q. & Liu, R. (2021). Flexural performance and toughness characteristics of geogrid-reinforced pervious concrete with different aggregate sizes. *Materials*, 14 (9), 2295. <https://doi.org/10.3390/ma14092295>
- Mohammed, S. I. & Najim, K. B. (2020). Mechanical strength, flexural behavior and fracture energy of Recycled Concrete Aggregate self-compacting concrete. *Structures*, 23, 34–43. <https://doi.org/10.1016/j.istruc.2019.09.010>
- Muda, Z. C., Malik, G., Usman, F., Beddu, S., Alam, M. A., Mustapha, K. N., Birima, A. H., Zarroq, O. S., Sidek, L. M. & Rashid, M. A. (2013). Impact resistance of sustainable construction material using light weight oil palm shells reinforced geogrid concrete slab. *IOP Conference Series: Earth and Environmental Science*, 16, 012062. <https://doi.org/10.1088/1755-1315/16/1/012062>
- Nishanthi, P., Vidjeapriya, R., Sivaram, S., Sathish, K., Bharath, K. & Muhammed Mukhthar Khan, M. K. (2021). Effect of geo-grid and steel fibres on flexural behaviour of reinforced concrete beams. *Materials Today: Proceedings*, 47, 4597–4605. <https://doi.org/10.1016/j.matpr.2021.05.452>

- Ou, Y. C., Tsai, M. S., Liu, K. Y. & Chang, K. C. (2012). Compressive behavior of steel-fiber-reinforced concrete with a high reinforcing index. *Journal of Materials in Civil Engineering*, 24 (2), 207–215. <https://ascelibrary.org/doi/10.1061/%28ASCE%29MT.1943-5533.0000372>
- Su, N. & Fan, X. (2021). Experimental Study on Flexural Toughness of Steel-Polyvinyl Alcohol Hybrid Fiber Reinforced Concrete. *IOP Conference Series: Earth and Environmental Science*, 719 (2), 022080. <https://doi.org/10.1088/1755-1315/719/2/022080>
- Vijay, T. J., Kumar, K. R., Vandhiyan, R., Mahender, K. & Tharani, K. (2020). Performance of geogrid reinforced concrete slabs under drop weight impact loading. *IOP Conference Series: Materials Science and Engineering*, 981 (3), 032070.
- Vijay, T. J., Raj, A. V. S. & Babu, M. S. (2021). Experimental investigation of concrete beams reinforced with polypropylene bars. *Materials Today: Proceedings*, 37, 1654–1658. <https://doi.org/10.1016/j.matpr.2020.07.181>
- Yousif, M. A., Mahmoud, K. S., Abd Hacheem, Z. & Rasheed, M. M. (2021). Effect of geogrid on the structural behavior of reinforced concrete beams. *Journal of Physics: Conference Series*, 1895 (1), 012048. <https://doi.org/10.1088/17426596/1895/1/012048>
- Yahaghi, J., Muda, Z. C. & Beddu, S. B. (2016). Impact resistance of oil palm shell concrete reinforced with polypropylene fibre. *Construction and Building Materials*, 123, 394–403. <https://doi.org/10.1016/j.conbuildmat.2016.07.026>
- Ye, Y., Liu, J., Zhang, Z., Wang, Z. & Peng, Q. (2020). Experimental study of high-strength steel fiber lightweight aggregate concrete on mechanical properties and toughness index. *Advances in Materials Science and Engineering*, 2020, 1–10. <https://doi.org/10.1155/2020/5915034>

## Summary

**Residual strength and toughness after impact loading for RC slabs strengthened with different layers of geogrid.** This study presents an experiment for investigating the residual strength and toughness of reinforced concrete, RC, and slab reinforced by a geogrid as shrinkage reinforcement along with lower tensile steel reinforcement. Three different parameters were considered: slab thickness, number of geogrid layers, and thickness of the upper concrete cover. Fifteen slab samples with sizes of 50 × 50 cm exposed to the impact load on its center before being re-loaded by the static load and six slab samples exposed to the static load only. The load and deflection relation were recorded through the static loading process for all specimens, where loading capacity, toughness, and toughness index were measured. The results show an enhancement in the slabs residual strength as the slab thickness and concrete cover increased. On the other hand, the residual strength of slabs has a remarkable decrease with the increase in geogrid layers. Moreover, the toughness has a positive relation with the concrete cover and has an inverse relation with the slab thickness and the number of layers. A geogrid reduced the number and distribution of cracks and mitigated their severity, especially for double layers with the same concrete cover.